THE ORIGIN OF THE «N2» ABSORPTION BAND
IN NATURAL YELLOW DIAMONDS

GORDON DAVIES

Wheatstone Physics Laboratory, King's College.
The Strand, London WC2R 2LS, U.K.

ABSTRACT — The N2 band, which is partly responsible for the yellow colour of many natural diamonds is shown to correlate in strength with the well-known N3 band, and to occur at a centre with the same symmetry. Assuming the N2 and N3 bands are transitions at the same optical centre it is shown that the shape of the N2 band and the relative strengths of the N2 and N3 bands are consistent with the N2 band being a forbidden transition which is made allowed by vibronic coupling with the N3 band.

1 — INTRODUCTION

The majority of diamonds are brown or yellow in colour. These colours may be produced by a variety of crystal defects, such as the «H3» centre (a defect composed of two substitutional nitrogen atoms and a vacancy [1]), or the single substitutional nitrogen atom characteristic of «type I b diamond» [2], or the «2.6 eV» centre (whose structure is unknown [3]), or the «N3» centre. This paper is concerned solely with the N3 centre. Its presence in a diamond may be identified by its characteristic absorption spectrum (Fig. 1). There is a sharp zero-phonon line observed at 24080 cm^{-1} (2.985 eV) and a series of phonon side-bands stretching to higher energy. To lower energy lies the «N2» band. Although the N2 band has significantly smaller absorption than the N3 band, the N2 band absorbs light which is visible to the human eye, while the N3 band absorbs mainly in the near ultraviolet part of the spectrum. As a result, both the N2 and N3

bands contribute about equally to giving the diamond its perceived yellow colour. From a gemmological point of view the N2 band is therefore an important feature of a diamond, even though it is a relatively weak contributor to the absorption spectrum. This paper presents the results of the first detailed scientific study of the N2 band.
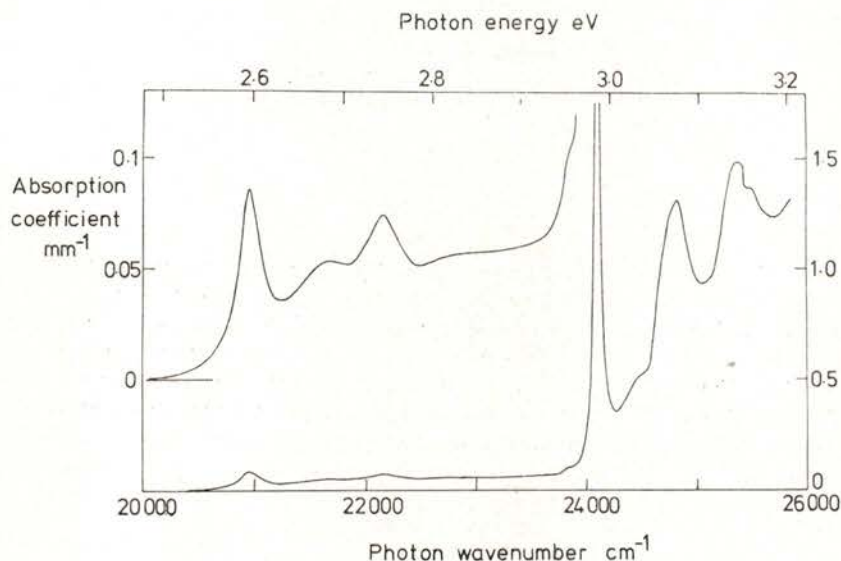

Fig. 1 — The absorption spectrum of a yellow diamond showing the N2 and N3 bands, measured at liquid nitrogen temperature. The N2 band is also shown magnified ten times.

Many studies have established that the N3 band is caused by an electric-dipole transition from a non-degenerate orbital ground state to a doubly degenerate excited state of an optical centre with C_{3v} symmetry [4], [5], [6]. An electron paramagnetic resonance signal is produced by an electron spin of a half at the N3 centre [7], [8], [9] and from this EPR spectrum it has been suggested that the N3 centre is composed of three nitrogen atoms all bonded to one common lattice site [10]. The model is consistent with the C_{3v} symmetry of the N3 centre deduced from the optical data. The presence of nitrogen is also consistent with the observations that the N3 centre may be synthesised when

nitrogen is made to migrate through a diamond during high temperature experiments [11].

When excited by near ultraviolet radiation the N3 centre emits a blue photoluminescence, with a spectrum which is approximately a mirror-image of the absorption band [12]. The radiative decay time [13] of the N3 luminescence is affected by the presence of pairs of substitutional nitrogen atoms in the diamonds. Allowing for this, the intrinsic decay time of the N3 centre is 41 ± 1 ns at low temperature (T < 400 K). At higher temperature the decay time becomes shorter, being less than 10 ns at T > 700 K. Even at low temperatures the luminescence efficiency of the N3 centre is only 0.3 (in the absence of extrinsic quenching by the pairs of nitrogen atoms). Thomaz and Davies [13] have suggested that these results arise because the electrons excited to the E level of the N3 centre are metastable and may de-excite to a non-radiative level of the N3 centre. At very low temperature it was assumed that tunnelling could occur between the E state and the nonradiative state, and at high temperature the electrons could be excited thermally over the energy barrier between the two states. The non-radiative state was postulated to be the excited state of the N2 absorption band. No resonant luminescence has been detected from this band — it is therefore non-radiative (for some as yet unspecified reason) as required by these ideas. It was suggested [13] that the N2 band is non-radiative because it is an electric-dipole forbidden transition; that is, the non-radiative nature of the N2 band is a feature intrinsic to the transition and is not the result of a fast non-radiative decay to other levels. This suggestion was based on a qualitative inspection of the N2 spectrum. In contrast to the N3 band and almost all electronic transitions seen in diamond [14], [15], the N2 band does not have a sharp zero-phonon line at its low energy side (Fig. 1). Instead only broad structure is observed, reminiscent of phonon sidebands. This structure could be caused by a transition to the N2 electronic level plus a vibration, the role of the vibration being to introduce deformations in the centre which mix together the N2 and N3 electronic states, thereby transferring absorption from the N3 band to the N2 band. This model can only work if the N2 and N3 bands occur at the same optical centre.

The first stage in investigating the N2 band is therefore to establish if it occurs at the N3 centre. In § 3 data are presented

which confirm that the two bands correlate in intensity with each other. In §§ 4, 5 uniaxial stress measurements are reported which show that the N2 band occurs at a trigonal optical centre, as does the N3 band. Assuming then that the N2 band is a forbidden transition at the N3 centre, we must investigate whether it is reasonable for the N2 band to be induced at its observed intensities by a vibronic mixing with the N3 states. The theory and calculations are presented in § 6 and shown, in § 7, to be consistent with the observed spectra.

2 — EXPERIMENTAL DETAILS

Natural diamonds were used throughout this study, and all the measurements were made with the specimens at liquid nitrogen temperature. The diamonds were chosen to be apparently homogeneously coloured to the naked eye. For the correlation data of Fig. 2, below, the N2 and N3 bands were measured through the same section of each specimen. Typical variations in band-strengths in different regions of the diamonds was ± 5 %, on a scale of several micro-metres. For the uniaxial stress measurements, the diamonds were polished to cubes of about 1.5 mm edges, with either (001), (110), (1$\overline{1}$0) faces or (111), (1$\overline{1}$0), (11$\overline{2}$) faces. The spectra were analysed using a Spex 1701 monochromator fitted with a DC-operated photomultiplier.

3 — N2, N3 CORRELATION

Measurement of the strength of the N2 band is straightforward since all its features are wide (at least 200 cm^{-1}, 25 meV) and so they are negligibly broadened by the random strain fields present in all diamonds (e.g. as a result of substitutional pairs of nitrogen atoms [16]) and which vary from one specimen to another. The peak absorption coefficient at the lowest energy N2 feature is therefore an adequate measurement of the N2 band. (This feature is at 20940 cm^{-1}, 2.596 eV). To measure the N3 bandstrength it is convenient to use the zero-phonon line, integrating its absorption coefficient to allow for the variable line-

width in different diamonds. The data have been expressed in terms of the zeroth moment of the line:

$$M_o = \int dv \ a(v) / v$$

where $a(v)$ is the absorption coefficient in mm^{-1} at photon wavenumber v. In practice the zero-phonon line is often too intense for its peak absorption to be measured accurately. Then the absorption coefficient at the minimum near 25000 cm^{-1} (3.10 eV) has been used instead and converted into a zero-phonon strength by means of the calibration data of Fig. 2a. This is an adequate procedure as long as there is no background wave-length-dependent absorption in the specimens (as there is in many brown diamonds [3], for example). The non-linearity in Fig. 2a is caused by the errors in measuring very strongly absorbing zero-phonon lines.
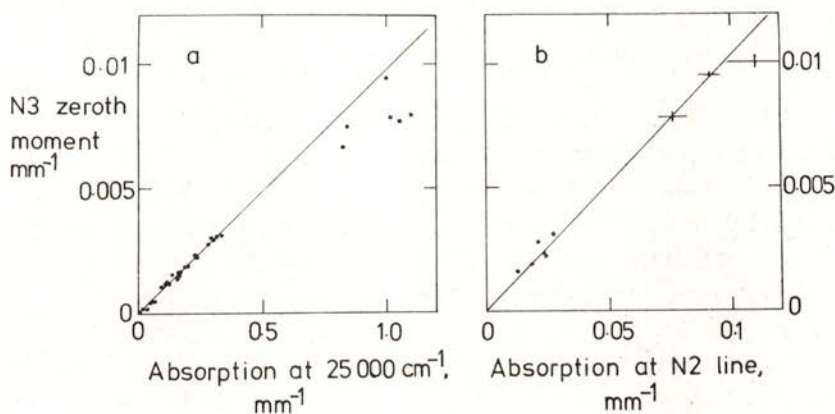

Fig. 2 — *a*) Correlation of the N3 absorption in the zero-phonon line and at the minimum of absorption near 25000 cm^{-1} (3.10 eV), measured at liquid nitrogen temperature. *b*) Correlation of the N2 and N3 absorption in nine specimens measured at liquid nitrogen temperature. The data of figure 2, are based on a re-analysis of spectra taken for reference [8].

Fig. 2b shows the results of the N2/N3 correlation for nine specimens. The correlation coefficient is 0.995. These measurements confirm a similarly high correlation observed between the N2 and N3 bands in eighteen diamonds by Clark et al [17].

From the spectra we may estimate the strength of the N2 band relative to the N3 band. Clearly from Fig. 1 the N3 band is probably superimposed on the high energy tail of the N2 band, and there is no way of separating the two bands using the absorption spectrum. (In fact, if the vibronic model outlined in § 1 is correct, there is no distinction between the N2 band and the N3 band: they are both parts of the same vibronic bandshape.) However, it is possible to measure the strength of absorption in the N2 band which lies on the low energy side of the N3 zero-phonon line, and also we can measure (as the «N3 strength») the absorption in the N2/N3 system on the high energy side of the N3 line. The two zeroth moments are related by:

$$M_{N2} / M_{N3} = \int_{20000}^{23800} d\nu \ a(\nu) \ \nu^{-1} / \int_{23800}^{29000} d\nu \ a(\nu) \ \nu^{-1} \quad (1)$$

$$= 0.046 \pm 0.004$$

4 — UNIAXIAL STRESS MEASUREMENTS

The effect of uniaxial compressions on the N3 zero-phonon line was reported by Crowther and Dean [5]. Data taken in this study (Fig. 3a) are in close agreement with that earlier work. The N2 line at 20940 cm^{-1} (2.596 eV) responds to stresses as shown, for the first time, in Fig. 3b. These data must be interpreted remembering that the full width at half height of the N2 line is 200 cm^{-1} (25 meV). Consequently the apparent splitting of the line under < 001 > compression (Fig. 3b) is not reliable (it does not exceed 1/20 of the linewidths). On the other hand at the highest < 111 > stresses the N2 line observed with electric

---

Fig. 3 (next page) — Energies of the stress-split components of (a) the N3 zero-phonon line (upper diagrams), and (b) the N2 line (lower diagrams), taken at liquid nitrogen temperature under < 001 >, < 111 > and [110] compressions. Crosses show data taken with electric vector **v** of the light parallel to the stress **s**, circles are for **v** $\perp$ **s**. For the N3 data with **s** $\parallel$ [110], closed circles are for **v** $\parallel$ [1$\bar{1}$0] and open circles for **v** $\parallel$ [001]. For the N2 data with **s** $\parallel$ [1$\bar{1}$0], **v** is $\parallel$ [1$\bar{1}$1]. The lines show the least squares fit of the Hamiltonian (equation 2) with the matrix elements listed in Table 1. N2 data labelled 'd' are predicted to be at the mean of lines c and e.
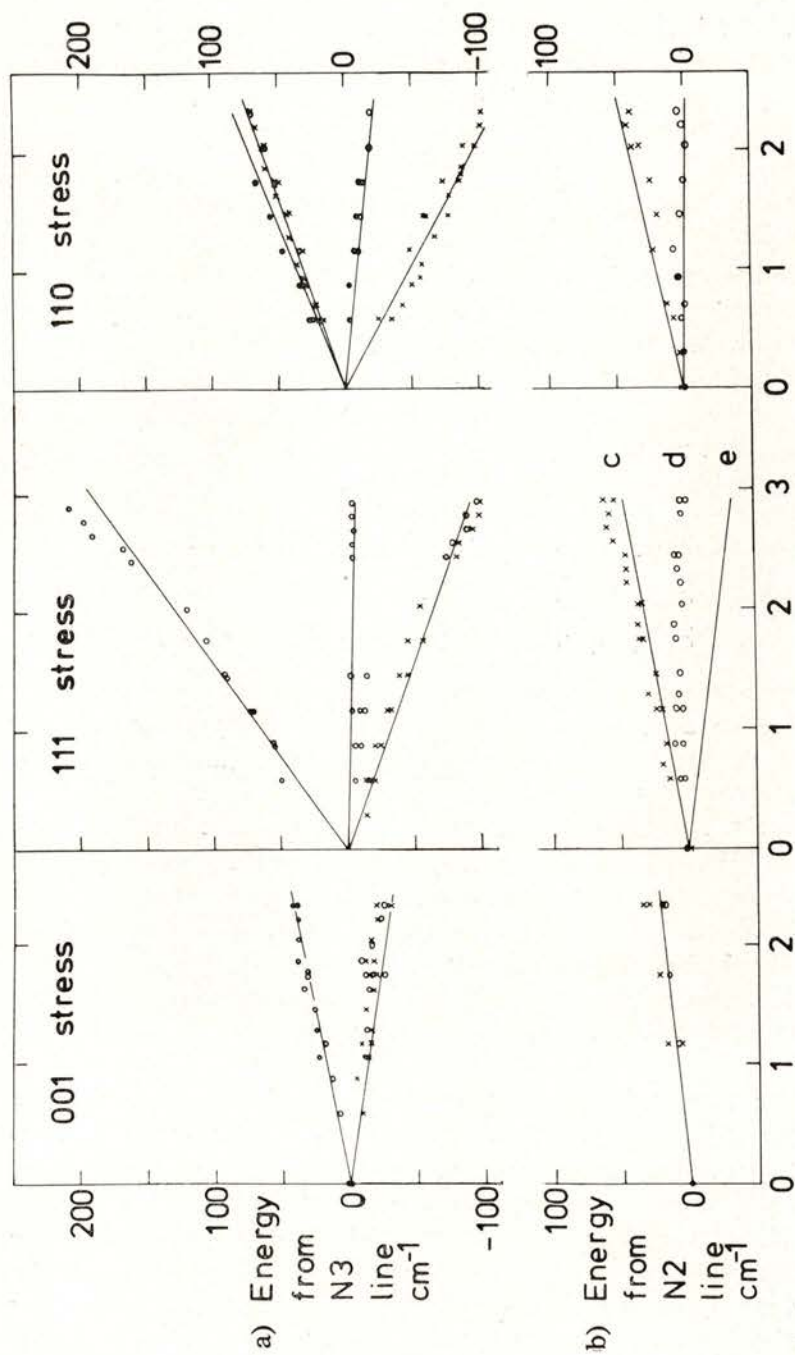
Fig. 3 — Effect of uniaxial compression (in G Pa); detailed caption in facing page.

vector $\mathbf{v}$ of the light polarised perpendicular to the stress axis $\mathbf{s}$ was 15 cm^{-1} wider than the N2 line observed with $\mathbf{v} \parallel \mathbf{s}$. Assuming a Lorentzian lineshape for the N2 line, this implies an unresolved splitting of about 50 cm^{-1} in the $\mathbf{v} \perp \mathbf{s}$ spectrum.

5 — ANALYSIS OF THE UNIAXIAL STRESS DATA

A trigonal optical centre like the N3 centre may have its main three-fold axis directed along any of the $< 111 >$ axes of the diamond. One orientation has the three-fold axis along [111]: we will define this to be the Z axis of that centre. The X and Y axes are chosen to lie along $[1\bar{1}2]$ and $[1\bar{1}0]$ respectively. Y is normal to a reflection plane of the C_{3v} centre. The Hamiltonian of the centre can then be written [18]:

$$
\begin{aligned}
H = H_o &+ c_{A1}\ (s_{xx} + s_{yy} + s_{zz}) + c'_{A1}\ (s_{xy} + s_{yz} + s_{zx}) \\
&+ c_{EX}\ (s_{xx} + s_{yy} - 2\,s_{zz}) + c_{EY}\ \sqrt{3}\ (s_{xx} - s_{yy}) \\
&+ c'_{EX}\ (s_{yz} + s_{zx} - 2\,s_{xy}) + c'_{EY}\ \sqrt{3}\ (s_{yz} - s_{zx})
\end{aligned}
\tag{2}
$$

Here H_o is the Hamiltonian at zero stress. The stress tensor components s_{ij} are defined with respect to the crystal axes x, y, z of the diamond. The electronic operators $c_{A1},..., c'_{EY}$ transform under the operations of the C_{3v} point group as shown by their subscripts. The lines on Fig. 3a show the least squared deviation fit of the Hamiltonian (equation 2) to the experimental data for the N3 line, assuming it to be an electric dipole allowed transition between an orbitally non-degenerate ground state and an orbitally doubly degenerate excited state (§ 1). The matrix elements of the $c_{A1},..., c'_{EY}$ operators are listed in Table 1. These results are closely in agreement with those of Crowther and Dean [5].

The results for the N2 line are more difficult to analyse because of the large width of the line (200 cm^{-1}, 25 meV, at zero stress). However, there is no resolved splitting with stress along $<001>$ in contrast to the results for $<111>$ and $<110>$ stresses (Fig. 3b). This suggests that the N2 optical centre also has trigonal symmetry (so that all orientations of the centre make the same angle with the [001] stress axis, and so are equally perturbed.) Further, since an orbitally degenerate state at a trigo-

TABLE 1 — Matrix elements of the operators $c_{A1}, \ldots, c'_{EY}$ of equation (2) derived from least squares fits to figure 3.

a) N3 zero-phonon line.

Matrix element	This work	Reference [5]
$< EX \mid c_{A1} \mid EX > - < A1 \mid c_{A1} \mid A1 >$	2	4
$< EX \mid c'_{A1} \mid EX > - < A1 \mid c_{A1} \mid A1 >$	62	69
$< EY \mid c_{EX} \mid EY >$	8	9
$< EY \mid c'_{EX} \mid EY >$	10	12

Units are cm^{-1} $(GPa)^{-1}$, typical uncertainty ± 4 cm^{-1}. $\mid EX >$, $\mid EY >$ are the zero-phonon levels of the E electronic states, $\mid A1 >$ the zero-phonon level of the A_1 ground electronic state.

b) N2 line, N2 excited state as an A_1 state.

$< a1 \mid c_{A1} \mid a1 > - < A1 \mid c_{A1} \mid A1 >$	8 cm^{-1} $(GPa)^{-1}$
$< a1 \mid c'_{A1} \mid a1 > - < A1 \mid c'_{A1} \mid A1 >$	13 cm^{-1} $(GPa)^{-1}$

Here $\mid a1 >$ is the excited state of the N2 line, $\mid A1 >$ its ground state.

c) N2 line, N2 excited state as an A_2 state.

$< A2 \mid c_{A1} \mid A2 > - < A1 \mid c_{A1} \mid A1 >$	9.5 cm^{-1} $(GPa)^{-1}$
$< A2 \mid c'_{A1} \mid A2 > - < A1 \mid c_{A1} \mid A1 >$	-21 cm^{-1} $(GPa)^{-1}$

Here $\mid A2 >$ is the excited state of the N2 line, $\mid A1 >$ its ground state.

nal centre is split by a $< 001 >$ stress [18] we conclude that both the ground and excited states of the N2 line are non-degenerate, or that if they are degenerate, the degeneracy is difficult to lift through applied stresses.

At a trigonal centre a transition between non-degenerate states is allowed when the electric vector of the light is parallel to the trigonal axis [19] (i. e. the Z axis as defined above). For this case, the least squares fit of the Hamiltonian (equation 2) to the data in Fig. 3b yields a close fit with the matrix elements listed in Table 1b. However, if the N2 line is an allowed transition we have to explain the lack of luminescence from it, and (more difficult) the extreme width of the line.

Portgal. Phys. — Vol. 12, fasc. 3-4, pp. 241-261, 1981

249

As an alternative we consider the N2 line to be a forbidden transition between non-degenerate states at the N3 centre, as implied by the stress data of Fig. 3b and the correlation of Fig. 2b. In this model the N2 transition is allowed through vibronic mixing with the N3 level (§ 1). Since the N3 transition is an allowed electric dipole transition between non-degenerate and doubly-degenerate states it occurs when the electric-vector of the light is polarised perpendicular to the trigonal axis of the centre (i. e. in the XY plane as defined above). The N2 transition is then expected to split under stress as expected for a «σ» oscillator at a trigonal centre, in Kaplyanskii's notation [19]. Under < 111 > stress *two* stress-split components are predicted [19] when the electric vector **v** of the light beam is perpendicular to the stress axis **s**. In the experiment only one component is resolved (Fig. 3b) although from the linewidths it is likely that there are two unresolved components (§ 4). Assuming that the observed line is at the mean position of the two predicted stress-split components, the least squares fit of the Hamiltonian (equation 2) to the data yields the fit shown in Fig. 3b with the parameters of Table 1c. Inspection of this fit shows that two lines expected with **v** ⊥ **s** for **s** ∥ < 111 > would indeed not be resolved.

The uniaxial stress data are thus consistent with the N2 line occurring at a trigonal centre, between non-degenerate orbital electronic states but with an electric dipole in the XY plane perpendicular to the trigonal axis of the centre. This assignment is in agreement with the model of § 1 in which the N2 band is vibronically induced from the N3 band. (An XY dipole transition between non-degenerate electronic states does not violate group theory selection rules because the N2 excited state is interpreted as a *vibronic* state which transforms as the E irreducible representation: see § 6 below.)

6 — A VIBRONIC MODEL

The data presented in § 4 and § 5 are consistent with the model that the N2 transition is an electric-dipole forbidden transition and is observed through vibronic mixing with the N3 transition. In this section we will investigate a simple model which

describes the interaction, to see if the order of magnitude of the parameters used in the model are plausible.

For definiteness we assume that the ground state of the N3 line transforms as A_1 in the C_{3v} point group, and that the N2 level is an A_2 state: the transition from A_1 to A_2 is electric dipole forbidden in C_{3v} symmetry [20]. The doubly degenerate N3 excited state must transform as E. Next we specify the relevant phonons at the optical centre. The dominant phonons observed in the N3 vibronic bands are the totally symmetric phonons [21]. However these are incapable of making the A_2 and E electronic states interact. For the vibronic mixing we must consider E modes of vibration at the centre. These E modes can produce a Jahn-Teller effect in the E states, and Thomaz and Davies [13] suggested that the radiative decay time measurements on the N3 band gave evidence for a weak Jahn-Teller relaxation. We will therefore consider the interaction of the A_2 and E electronic states brought about by *one* E mode of vibration which can also produce a Jahn-Teller effect in the E electronic state. By considering only one E mode, and by ignoring all the A_1 modes, we can minimise the number of parameters required by theory, although at the expense of realism.

If we switch off the interaction between the A_2 and E states, and also switch off the Jahn-Teller effect in the E states, we can write the vibronic states as Born-Oppenheimer products of electronic states (denoted by ϕ) and harmonic vibrational states (denoted by χ):

$$
\begin{aligned}
\psi_{A1pq}(r, Q_X, Q_Y) &= \phi_{A1}(r)\, \chi_p(Q_X)\, \chi_q(Q_Y) \\
\psi_{A2pq}(r, Q_X, Q_Y) &= \phi_{A2}(r)\, \chi_p(Q_X)\, \chi_q(Q_Y) \\
\psi_{EXpq}(r, Q_X, Q_Y) &= \phi_X(r)\, \chi_p(Q_X)\, \chi_q(Q_Y) \\
\psi_{EYpq}(r, Q_X, Q_Y) &= \phi_Y(r)\, \chi_p(Q_X)\, \chi_q(Q_Y)
\end{aligned}
\tag{3}
$$

Here, Q_X and Q_Y represent the vibrational coordinates in the E mode, and r represents the electronic coordinates. The integers p, q are the mode occupation numbers. The adiabatic potentials in the A_1, A_2 and E states are

$$
V = W_i + \tfrac{1}{2}\, m\, \omega^2 (Q_X^2 + Q_Y^2)
\tag{4}
$$

where W_i is the energy of the relevant electronic state, $\hbar\omega$ is the quantum of the E vibrational mode and m is its reduced mass. We now introduce the additional terms:

$$V' = d_X Q_X + d_Y Q_Y \qquad (5)$$

into equation 4. The electronic operators d have matrix elements between the A_2 and E electronic states of

$$-\int dr\ \phi_X^* d_X \phi_X = \int dr\ \phi_Y^* d_X \phi_Y = \int dr\ \phi_X^* d_Y \phi_Y = \int dr\ \phi_Y^* d_Y \phi_X = k$$

$$(6a)$$

and

$$\int dr\ \phi_X^* d_Y \phi_{A2} = -\int dr\ \phi_Y^* d_X \phi_{A2} = \int dr\ \phi_{A2}^* d_Y \phi_X = -\int dr\ \phi_{A2}^* d_X \phi_Y = c$$

$$(6b)$$

with all other terms zero. These operators, which describe the perturbations produced by atomic movements Q_X, Q_Y, are related through the elastic constants, to the operators $c_{EX},...,\ c'_{EY}$ which describe perturbations produced by stresses. The important difference between the vibronic mixing and the stress perturbation is that the vibronic term depends linearly on the vibrational coordinates Q_X, Q_Y while the stress perturbation is independent of the vibrational coordinate. Matrix elements of the stress perturbation taken between the uncoupled states of equation (3) are only non-zero for states of the same vibrational quantum numbers. Matrix elements of V', the vibrational coupling, exist only between the uncoupled states of equation (3) which differ by one in one of the vibrational occupation numbers: For example the term $d_X Q_X$ has non-zero matrix elements between the uncoupled states of equation (3) of:

$$\int dr\ dQ_X\ dQ_Y\ \psi_{EXpq}^*\ d_X Q_X\ \psi_{EX,p+1,q} = -k\ [(p+1)\ \hbar/(2m\omega)]^{\frac{1}{2}}$$

$$(7)$$

$$\int dr\ dQ_X dQ_Y \psi_{A2pq}^*\ d_X Q_X\ \psi_{EY,p+1,q} = -c\ [(p+1)\ \hbar/(2m\omega)]^{\frac{1}{2}}$$

The Jahn-Teller relaxation energy S_{Exe}, measured in units of $\hbar\omega$, of the E electronic state due solely to the effect of V' on the EX and EY electronic states is:

$$S_{Exe} = k^2/2m\hbar\omega^3 \qquad (8)$$

Similarly we define a parameter S_{AE} to describe the interaction of the A_2 and the E electronic states as:

$$S_{AE} = c^2/2m\hbar\omega^3 \qquad (9)$$

The problem has now been reduced to determining the eigenvectors and eigenvalues of the secular matrix given by expressions like equations (6) to (9) in terms of the uncoupled basis states of equation (3). The calculations have been carried out using the parameters contained in reference [13]: i.e. with $S_{Exe} = 0.69$ and with the energy difference (W_E-W_{A2}) of the electronic states at $Q_X = Q_Y = 0$ (equation 4) being $W_E-W_{A2} = 4.625\ \hbar\omega$. The energy origin was defined at $W_E = 0$. Results are given in Figs. 4 to 6
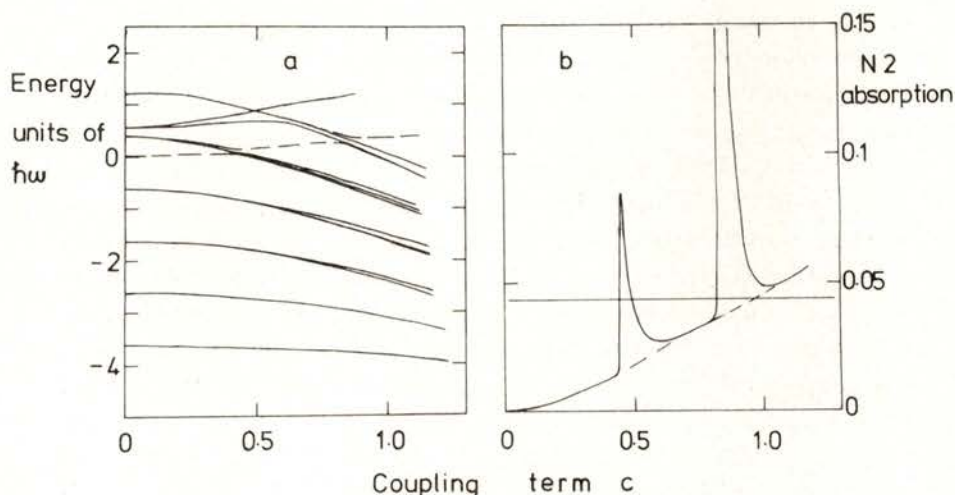

Fig. 4 — a) Lowest energy vibronic levels for the model of § 6. Parameters used are: $k = 1.17$, $m = 1$, $\hbar\omega = 1$, $W_E = 0$, $W_{A2} = -4.625$. Broken line shows N3 «zero-phonon» state. b) Intensity of all the transitions with energies less than the N3 zero-phonon line, using the parameters as in (a). The N3 zero-phonon line was formally defined as the lowest energy transition with over 0.2 of the total absorption. The horizontal line shows the value derived from equation (1).

as functions of the coupling c. Fig. 4a shows the energy levels for the lowest vibronic states. With increasing S_{AE} the N2 levels move to lower energy. Qualitatively this movement may be thought of as arising from the repulsion of the 'N2' levels as the interaction between them is increased. More quantitatively we can get some insight into the behaviour of this system by looking at the adiabatic potential surfaces given by equation (4) modified by equation (5). These potential surfaces are the solutions for V of the determinantal equation:

$$
\begin{vmatrix}
W_E + U - kQ_X - V & kQ_Y & cQ_Y \\
kQ_Y & W_E + U + kQ_X - V & -cQ_X \\
cQ_Y & -cQ_X & W_{A2} + U - V
\end{vmatrix} = 0
$$

(10)

where U denotes $\frac{1}{2} m\omega^2 (Q_X^2 + Q_Y^2)$. Cross-sections through the surfaces and computed energy levels are shown in Fig. 5.

The repulsion of the 'N2' and 'N3' levels as S_{AE} increases causes sucessive vibronic levels of the 'N2' set to cross the 'N3' zero-phonon level (Fig. 4a). At these crossing points there is a particularly large effect on the calculated shape of the absorption spectrum (Fig. 6). The spectra have been calculated from the eigenvectors of the vibronic secular equation. Light polarised along the X axis of the optical centre (as defined in § 5) can induce transitions only from the state ψ_{A100} to ψ_{EX00} when the vibronic interaction V' is switched off. At 0 K and V' = 0 this would be the only transition allowed, in this model. With V' $\neq$ 0 the vibronic eigenstates are linear combinations of the uncoupled states $\psi_{A2pq} \cdots \psi_{EYpq}$. Transitions with X polarised light can then occur from ψ_{A100} to any vibronic state which contains an admixture of ψ_{EX00}. The relative intensity of the transition is simply the square of the coefficient of the ψ_{EX00} term in the linear combination.

From experiment we know the strength of the N2 band relative to the N3 band (equation 1). Similarly we may calculate the total absorption strength predicted to lie at energies below the N3 zero-phonon line in spectra like Fig. 6. The result, Fig. 4b, shows a series of peaks at the resonance conditions when the
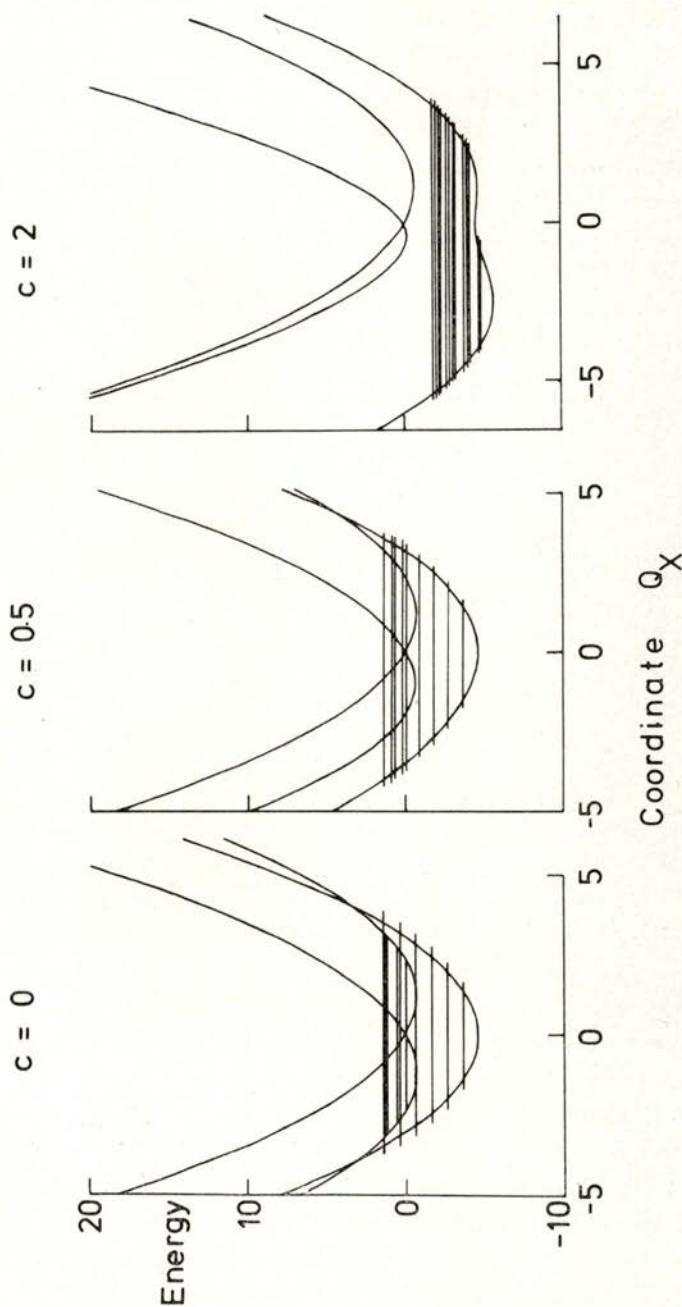
Fig. 5 — Cross-sections through the adiabatic potentials (equation 10) along the Q_X axis with $Q_Y = 0$. Parameters are $m = 1$, $\hbar\omega = 1$, $W_{A2} = -4.625$, $k = 1.17$. At left the N3 state undergoes a Jahn-Teller distortion without interacting with the N2 level ($c = 0$). The centre shows weak interaction ($c = 0.5$) and at right strong interaction ($c = 2.0$). The vibronic energy levels are shown by horizontal lines. The lowest energy level is the non-degenerate N2 zero-phonon level with weak coupling, and is a near degenerate triplet with strong coupling as three minima are formed in the adiabatic potential.

'N2' vibronic levels coincide with the 'N3' zero-phonon level. In reality there is not a single E vibrational mode which interacts with the electronic states, and the vibronic coupling is spread out over a range of vibrational frequencies. Consequently these resonances will not occur to the extent shown on Fig. 4b: these large peaks are an artifact of this single mode model. However it would be reasonable to expect to see some small resonance effects near to the N3 zero-phonon line, and possibly the structure near 23800 cm^{-1} (2.950 eV) is caused by this mechanism.
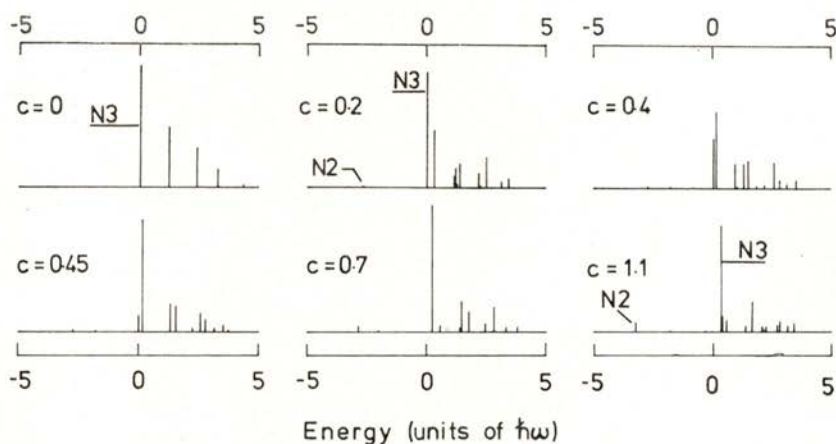

Fig. 6 — Calculated spectra with $m = 1$, $\hbar\omega = 1$, $W_E = 0$, $W_{A2} = -4.625$ and $k = 1.17$, for different values of c. Each of these lines is the «zero-phonon» line for a suitable progression of totally symmetric phonon sidebands.

Ignoring the resonance peaks on Fig. 4b, the required relative strengths of the N2 and N3 bands are obtained when $S_{AE} = 0.4$. The calculated bandshape is then as shown in Fig. 6. For comparison with experiment we have to imagine each of the spikes in Fig. 6 as acting as the 'zero-phonon' line for the progressions of totally symmetric phonons [21] which have been ignored in this model. There is, however, consistency with the measured spectrum of Fig. 1 in that the N2 band is predicted to have its strongest feature at the low energy side (the 'N2 line').

7 — SELF-CONSISTENCY CHECKS ON THE VIBRONIC MODEL

The model proposed for the origin of the N2 bands has the following properties in agreement with experiment:

i)   It requires the N2 and N3 transitions to occur at the same optical centre, and hence the N2 and N3 bandstrengths must correlate linearly with each other, as observed in Fig. 2b, and the symmetry of the N2 optical centre has to be the same as the symmetry of the N3 centre, since they are identical, and this has been demonstrated in § 5.

ii)   The N2 electronic transition is a forbidden electric-dipole transition. Therefore, after excitation into the N3 level, any de-excitation process which takes the centre into the N2 vibronic levels will lead to a strong quenching of the luminescence because the zero-phonon transition from the N2 zero-phonon state to the ψ_{A100} state remains forbidden even after allowing for the vibronic interaction. It is predicted from the model that weak luminescence transitions will occur near 18550 cm^{-1}, 2.3 eV, as the N2 zero-phonon level decays to the one phonon states ψ_{A110} and ψ_{A101}. These transitions are predicted to have less than 10^{-2} of the N3 luminescence transition probability and a width of 200 cm^{-1} (25 meV), since, like the N2 absorption line, they are transitions which create one of the E modes of vibration. Not surprisingly, these transitions are not convincingly observed in the low temperature luminescence spectrum.

To these general results we can add:

iii)   The calculated N2 absorption bandshape has the N2 line (i.e. the lowest energy feature) as the strongest line (Fig. 6), and this is as observed (Fig. 1).

iv)   The strength of the interaction required to produce the observed N2 bandstrength is $S_{AE} = 0.4$. The definition of S_{AE} was chosen in equation (9) to be analogous to a Huang-Rhys factor. At deep levels in diamond Huang-Rhys factors are typically of the order of unity, and in particular S values close to 0.5 are observed in the pseudo-Jahn-Teller distortions occurring at the H3

and H4 optical centres in diamond [15]. The vibronic coupling derived for the N2 and N3 levels is therefore typical for diamond.

v) The mixing of the uncoupled states of equation (3) leads to the observed N3 zero-phonon level containing some admixture from ϕ_{A2} This admixture lowers the probability of luminescence transitions from the N3 zero-phonon level to the ϕ_{A1} electronic state. From the calculations of § 6, and again smoothing out the resonance effects at the values of S_{AE} which give level crossing, the N3 luminescence decay time is predicted to be 10 % longer than the radiative lifetime of the pure ϕ_{EX} or ϕ_{EY} to ϕ_{A1} transition. This provides a small contribution to making the radiative decay time of the N3 luminescence decay time ($\tau = 150$ ns after allowing for the non-radiative decay to the N2 levels [13]) so much larger than the values reported for other electric dipole transitions in diamond (typically ~ 20 ns [22]).

A positive test of the vibronic model would come from applying a static deformation to the diamond so as to induce absorption transitions between the ϕ_{A1} electronic ground state and the N2 *zero-phonon* level. To a good approximation the N2 zero-phonon level is composed solely of the ψ_{A200} state of equation (3). The N2 one-phonon states (which are observed as the N2 line) are admixtures of the ψ_{A201} state with ψ_{EX00}, and the ψ_{A210} state with ψ_{EY00} (see equation 7). It is the ϕ_{EX} and ϕ_{EY} components which make the N2 line observable. With an applied static stress which transforms, say, as EX, the ψ_{A200} (N2 zero-phonon) state interacts with the ψ_{EY00} component of the ψ_{A210}, ψ_{EY00} (N2 one-phonon) state, transferring intensity to the N2 zero-phonon line. Additional mixing occurs directly between the N2 and N3 zero-phonon lines. The experiment consists of applying measured *stresses* to the diamond while the known parameter S_{AE} in the vibronic model refers to atomic movements Q_X, Q_Y (equations 5, 6, 9) at the N2/N3 optical centre. To estimate the size of the induced N2 zero-phonon line we must therefore convert the known parameter S_{AE} to a stress matrix element by means of a suitable elastic constant which will differ from the known elastic constants of diamond because of the presence of the optical centre. To do this we make the assumption that the elastic constants near the optical centre are the same for all the vibronic levels of he N2/N3 excited states. Now, the relaxation energies S_{AE}, S_{Exe} are

proportional to the squares of the matrix elements c and k (equations 6, 8, 9). Since, from Table 1,

$$< EY \,|\, c_{EX} \,|\, EY > \; \approx \; < EY \,|\, c'_{EX} \,|\, EY >$$

for the N3 states we estimate the interaction of the A2 and E *electronic* states by:

$$\int dr \, \phi^{*}_{A2} \, c_{EX} \, \phi_{EY} \sim \int dr \, \phi^{*}_{A2} \, c'_{EX} \, \phi_{EY} \sim (S_{AE}/S_{Exe})^{\frac{1}{2}} \int dr \, \phi^{*}_{EY} \, c_{EX} \, \phi_{EY}$$

The integral on the right is obtained from Table 1 for

$$\int dr \, \phi^{*}_{EY} \, c_{EX} \, \phi_{EY} = \; < EY \,|\, c_{EX} \,|\, EY > \cdot K(E)^{-1}$$

where $K(E)$ is the Ham reduction factor [23] with a value $K(E) = 0.6$ at $S_{Exe} = 0.69$. Hence $\int dr \, \phi^{*}_{EY} \, c_{EX} \, \phi_{EY} \sim 11 \; \text{cm}^{-1} \, (\text{GPa})^{-1}$. This value may be scaled into the vibronic secular matrix (§ 6) since we have already assumed that $\hbar\omega = 1186 \; \text{cm}^{-1}$. Thus $\int dr \, \phi^{*}_{EY} \, c_{EX} \, \phi_{EY} \sim 0.01 \, \hbar\omega \, (\text{GPa})^{-1}$. From the eigenstates of the vibronic secular matrix including a $< 001 >$ stress of 3 GPa the strength of the induced N2 zero-phonon line is predicted to be $\sim 10^{-4}$ of the total N2 and N3 absorption. Experiments to observe this line with $< 001 >$ stresses of up to 2.5 GPa applied at liquid nitrogen temperature have not shown detectable absorption, but an N2 zero-phonon line would only have been detected if its strength exceeded approximately 2×10^{-3} of the total absorption. No change in the N3 radiative decay time has been observed under $< 001 >$ stresses by M. F. Thomaz (private communication); and again the effect predicted by the theoretical model is very small.

Finally, the vibronic model discussed here has ignored the effects of totally symmetric modes. For the N3 zero-phonon line the largest stress response is given by the $< EX \,|\, c'_{A1} \,|\, EX >$ term (Table 1) which describes the perturbations produced by totally symmetric, volume-conserving compressions along the trigonal axis of each centre (i.e. stresses $2s_{ZZ}$-s_{XX}-s_{YY} in the coordinates defined at the beginning of § 5). This coupling is presumably

responsible for the N3 band being predominantly coupled to totally symmetric modes [21]. The totally symmetric perturbations of the N2 line are about three times smaller (Table 1c) implying a Huang-Rhys factor for the N2 totally symmetric coupling some 9 times smaller than for the N3 line. This is qualitatively as observed (Fig. 1): there are no pronounced phonon sidebands of the N2 line as there are for the N3 line.

The difference in the totally symmetric coupling for the N2 and N3 lines has an effect on the vibronic theory. The interaction of the ϕ_{A2} and ϕ_{EX}, ϕ_{EY} states is quenched by their relative displacements in the totally symmetric modes, analogous to a Ham reduction. However, the effect is not very large. Each vibronic matrix element (equation 7) is reduced by a factor determined by the overlap of the totally symmetric vibrational states. This factor will be less than about three for the vibronic states of interest and will not affect the general results given here.

8 — SUMMARY

Experimental data presented in this paper confirm that the strengths of the N2 and N3 absorption bands correlate with each other (Fig. 2). Uniaxial stress data on the N2 line have been shown to be consistent with it occurring at a trigonal centre (§ 5) as does the N3 line. The different magnitudes of the stress responses of the N2 and N3 lines are consistent with the different strengths of their phonon sidebands (§ 7). The suggestion [13] that the N2 line is a forbidden transition made allowed by vibronic interaction with the N3 level has been shown to be quantitatively reasonable (§ 6). Positive confirmation of this model has not been achieved. The theory predicts that the N2 zero-phonon line will be induced by stress, but will be too weak to observe, and experiments have not detected it. However the model does provide a natural explanation for the large width of the N2 line, and for the lack of luminescence observed from the N2 line (§ 7).

REFERENCES

[1] G. DAVIES, *J. Phys.*, **C9**, L537 (1976).
[2] H. B. DYER, F. A. RAAL, L. DU PREEZ and J. H. N. LOUBSER, *Phil. Mag.*, **11**, 763 (1965).

[3] A. T. COLLINS and K. MOHAMMED, *J. Phys.*, C14, in press.

[4] C. D. CLARK and C. A. NORRIS, *J. Phys.*, C3, 651 (1970).

[5] P. A. CROWTHER and P. J. DEAN, *J. Phys. Chem. Solids,* 28, 1115 (1967).

[6] A. A. KAPLYANSKII, V. I. KOLYSHKIN and V. N. MEDVEDEV, *Sov. Phys. Solid State,* 12, 1193 (1970).

[7] B. HENDERSON, *Industrial Diamond Review,* March 1980, pp. 92-97.

[8] G. DAVIES, C. M. WELBOURN and J. H. N. LOUBSER, *Diamond Research,* 1978, pp. 23-30.

[9] G. DAVIES and I. SUMMERSGILL, *Diamond Research,* 1973, pp. 2-5.

[10] M. YA SHCHERBAKOVA and E. V. SOBOLEV, *Dokl. Akad. Nauk. SSSR,* 204, 851 (1972); J. H. N. LOUBSER and A. C. J. WRIGHT, *Diamond Research,* 1973, pp. 16-20; M. YA SHCHERBAKOVA and V. A. NADOLINNYI, *Zhurnal Struct. Khimii,* 19, 305 (1978).

[11] R. M. CHRENKO, R. E. TUFT and R. M. STRONG, *Nature,* 270, 141 (1977); B. P. ALLEN and T. EVANS, *Proc. R. Soc.,* A375, 93 (1981).

[12] P. G. N. NAYAR, *Proc. Ind. Acad. Sci.,* A14, 1 (1941).

[13] M. F. THOMAZ and G. DAVIES, *Proc. R. Soc.,* A362, 405 (1978).

[14] J. WALKER, *Rep. Prog. Phys.,* 42, 1605 (1979).

[15] G. DAVIES, *Rep. Prog. Phys.,* 44, 787 (1981).

[16] G. DAVIES, *J. Phys.,* C3, 2474 (1970).

[17] C. D. CLARK, R. W. DITCHBURN and H. B. DYER, *Proc. R. Soc.,* A234, 363 (1956).

[18] A. E. HUGHES and W. A. RUNCIMAN, *Proc. Phys. Soc.,* 80, 827 (1967).

[19] A. A. KAPLYANSKII, *Opt. Spectrosc.,* 16, 329 (1964).

[20] M. TINKHAM, *Group Theory and Quantum Mechanics* (New York: McGraw-Hill) (1964).

[21] G. DAVIES, *J. Phys.,* C7, 3797 (1974).

[22] M. D. CROSSFIELD, G. DAVIES, A. T. COLLINS and E. C. LIGHTOWLERS, *J. Phys.,* C7, 1909 (1974); M. D. CROSSFIELD, PhD. thesis, University of London (1981).

[23] F. S. HAM, in *Electron paramagnetic resonance,* edited by D. Geshwind (New York: Plenum Press) (1972), pp. 1-119.